2018 Annual American Control Conference (ACC)
June 27–29, 2018. Wisconsin Center, Milwaukee, USA

Joint-Space Trajectory Optimization of a 7-DOF Baxter Using Multivariable Extremum Seeking

Mostafa Bagheri[1], Miroslav Krstić[2], and Peiman Naseradinmousavi[3]

Abstract— **In this paper, a novel analytical coupled trajectory optimization of a 7-DOF Baxter manipulator utilizing Extremum Seeking (ES) approach is presented. The robotic manipulators are used in network-based industrial units, and even homes, by expending a significant lumped amount of energy and therefore, optimal trajectories need to be generated to address efficiency issues. These robots are typically operated for thousands of cycles resulting in a considerable cost of operation. First, coupled dynamic equations are derived using the Lagrangian method and experimentally validated to examine the accuracy of the model. Then, global design sensitivity analysis is performed to investigate the effects of changes of optimization variables on the cost function leading to select the most effective ones. We examine a discrete-time multivariable gradient-based extremum seeking scheme enforcing operational time and torque saturation constraints in order to minimize the lumped amount of energy consumed in a path given. The results are compared with those of a global heuristic genetic algorithm to discuss the locality/globality of optimal solutions. Finally, the optimal trajectory is experimentally implemented to be thoroughly compared with the inefficient one. The results reveal that the proposed scheme yields the minimum energy consumption in addition to overcoming the robot's jerky motion observed in an inefficient path.**

I. Introduction

Robots are widely utilized in industry due to their reliable, fast, and precise motions although they are not energy-efficient and hence consume a significant lumped amount of energy. The energy consumption and subsequently cost of operation considerably increase when thousands of robots are working together, for example in a factory, to carry out a network-based task for thousands of cycles. Based on the recent statistics published, industries are among the largest consumers of energy in which the robots take the biggest share of consumption. It is worth mentioning that the robots used in auto industry consume more than half of the total energy required to produce a vehicle body. The total mechanical energy consumed by the robot is expectedly affected by the required torque of each joint in addition to the joints' angular velocities. The high level of energy consumption is typically caused by jerky motions of robots. Many research efforts addressed path planning and minimizing joints' torques. Some researchers have focused on path smoothness and/or minimizing the execution time, which may not necessarily yield a minimal amount of energy consumption.

Extremum Seeking (ES) is a model-free optimization approach [1]–[3] for systems with unknown dynamics and with a measurable output which has been applied to a wide range of technical applications [4]–[8]. The first proof of stability for an extremum seeking feedback scheme was provided by Krstić and Wang [2]. They utilized the tools of averaging and singular perturbations in revealing that solutions of the closed-loop system converge to a small neighborhood of the extremum of the equilibrium map. Note that the ES approach can yield fast convergence, in spite of being simple to implement by utilizing iterative (batch-to-batch) optimization of the cost function. Frihauf *et al.* [9] carried out optimization of a single-input discrete-time linear system using discrete-time ES.

Discrete-time extremum seeking with stochastic perturbation was studied without measurement noise in [10]. Stanković and Stipanović [11] investigated discrete-time extremum seeking with sinusoidal perturbation including measurement noise. Liu and Krstić [12], [13] and Choi *et al.* [14] employed discrete-time ES for one-variable static system with an extremum using stochastic and sinusoidal perturbations, respectively.

Rotea [15] and Walsh [16] studied multivariable extremum seeking schemes for time-invariant plants. Ariyur and Krstić [17] investigated, for the first time, the multivariable extremum seeking scheme for general time-varying parameters. Li *et al.* [18] utilized the multivariable ES in optimizing the cooling power of a tunable thermoacoustic cooler. Other multivariable ES applications can be found in [19]–[21].

Through this research effort, the time-invariant multivariable optimization of all joints' trajectories is presented in detail. To the best of our knowledge, the multivariable ES has not yet been utilized for the minimization of the energy consumed by robotic manipulators. The contribution of our work is in employing the multivariable gradient-based discrete-time ES scheme as follows:

1) The scheme is being numerically applied for a 7-DOF manipulator and the results implemented experimentally;
2) The scheme's computational burden is significantly less than other optimization methods including Genetic Algorithm (GA) which we examine here.

In order to carry out the operational optimization, fourteenth-

[1]Mostafa Bagheri is with the Department of Mechanical and Aerospace Engineering, San Diego State University and University of California San Diego, USA. http://peimannm.sdsu.edu/members.html, http://flyingv.ucsd.edu/mostafa

[2]Miroslav Krstić is with the Department of Mechanical and Aerospace Engineering, University of California San Diego, La Jolla, CA 92093, USA http://flyingv.ucsd.edu

[3]Peiman Naseradinmousavi is with the Department of Mechanical Engineering, San Diego State University, San Diego, CA 92115, USA http://peimannm.sdsu.edu

978-1-5386-5428-6/$31.00 ©2018 AACC

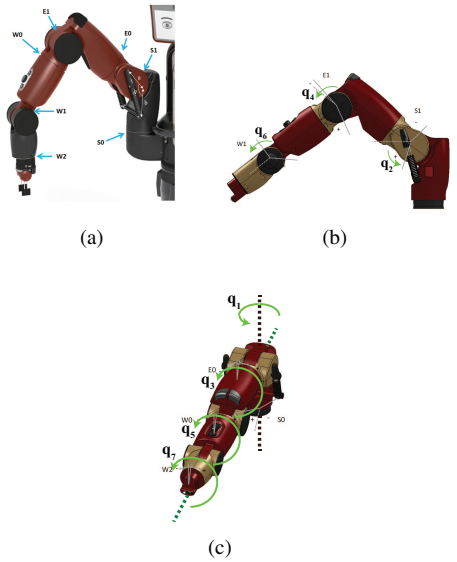

(a) (b) (c)

Fig. 1. (a) The 7-DOF Baxter's arm; The joints' configuration: (b) sagittal view; (c) top view

order dynamic equations using the Lagrangian method are derived. Then, the cost function is formulated as the lumped amount of mechanical energy consumption enforcing operational time and torque saturation constraints. The effects of changes of optimization variables on the cost function are studied using global design sensitivity analysis in order to select the most effective ones , and a nominal "*S-Shaped*" trajectory is fitted for every joint for a collision-free trajectory given. We utilize both Extremum Seeking and Genetic Algorithms to improve the dynamic characteristics of the fitted (nominal) trajectories along with minimizing the energy consumption. The optimal trajectory is experimentally implemented and thoroughly compared with the inefficient one.

II. Mathematical Modeling

The redundant manipulator, which is being studied here, has 7-DOF as shown in Fig. 1. The mass, Coriolis, and gravitational (stiffness) matrices are symbolically derived using the Euler-Lagrange equation:

$$D(q)\ddot{q} + C(q,\dot{q})\dot{q} + \phi(q) = \tau \qquad (1)$$

where, $\ddot{q}$ and τ indicate the vectors of angular acceleration and driving torque of the joints, respectively, and $\phi(q)$ is the gravitational vector $\phi_k = \frac{\partial P}{\partial q_k}$. The robot's Denavit-Hartenberg parameters are shown in Table I provided by the manufacturer. We implemented the symbolic formulations in MATLAB and obtained the coupled fourteenth-order nonlinear dynamic equations to be used in the optimization process [22], [23].

III. Trajectory Optimization

The undesirable responses can be observed through the experimental work which we have carried out in our Dynamic Systems and Control Laboratory (DSCL) [22], [23].

TABLE I

Baxter's Denavit-Hartenberg Parameters

Link	a_i	d_i	α_i	θ_i
1	0.069	0.27035	$-\pi/2$	θ_1
2	0	0	$\pi/2$	$\theta_2 + \pi/2$
3	0.069	0.36435	$-\pi/2$	θ_3
4	0	0	$\pi/2$	θ_4
5	0.010	0.37429	$-\pi/2$	θ_5
6	0	0	$\pi/2$	θ_6
7	0	0.3945	0	θ_7

TABLE II

The ranges of joints' angles (degree)

Joints's Name	Range	Initial Point	End Point
S_0	-97.5 to 90	-87.0532	-25.6510
S_1	-80 to 60	-50.0156	5.0300
E_0	-170 to 170	-10.1733	41.0350
E_1	0 to 150	20.1435	65.1590
W_0	-170 to 170	-30.1357	-85.2770
W_1	-90 to 115	9.2920	-46.2050
W_2	-170 to 170	-60.0735	12.0360

We observed that the robot collides with other objects close to the end point making the motion unreliable and inefficient. This is counted as a harmful dynamical behavior for both the industrial and home applications. Note that the Baxter, which is being analyzed here, has been designed for research purposes and hence has no predefined nominal trajectory. Therefore, the coupled trajectory optimization of the robot, as a part of the nonautonomous approach, is a necessity to be carried out in order to considerably reduce the mechanical energy consumption along with removing the jerky motions to avoid such a harmful collision discussed earlier.

The feasible joints' ranges along with the initial and end points are listed in Table II. Note that one of the physical constraints, which needs to be implemented in the optimization formulation, is zero angular velocity/acceleration at the initial and zero angular velocity at the end points, indicating that the manipulator would remain stationary at those points.

We fit the following nonlinear functions (nominal trajectories) [24]–[27] to the joints' actual trajectories which are generated with respect to the initial/end points given in Table II using the Baxter's PID controller:

$$\theta_i(k) = A_i \tanh(B_i(k\Delta t)^{C_i}) + D_i \qquad i = 1, \cdots, 7 \quad (2)$$

where, $k = 0, 1, \cdots, N$, Δt indicates constant time step, $t_f = N\Delta t$ (operation time), and A_i's, B_i's, C_i's, and D_i's are calculated utilizing the least square method for the trajectory fitting process listed in Table III. Note that we discretized the functions due to the discrete-time nature of the problem.

Note that the A_i's and D_i's are constant/unique parameters reported in [22], [23]. The B_i's and C_i's are the optimization

TABLE III
THE NOMINAL TRAJECTORIES' COEFFICIENTS

Joint's Name	A	$B \times 10^2$	C	D
S_0	61.4022	1.532	2.9430	-87.0532
S_1	55.0456	1.489	2.9760	-50.0156
E_0	51.2083	1.504	2.9385	-10.1733
E_1	45.0155	1.510	2.9712	20.1435
W_0	-55.1413	1.490	2.9910	-30.1357
W_1	-55.9970	1.513	2.9293	9.2920
W_2	72.1095	1.495	2.9382	-60.0735

variables although a crucial issue to address is the number of parameters expectedly leading to a cumbersome computational cost. Therefore, the sensitivity of the optimization process to the variables of B_i's and C_i's needs to be carefully addressed.

We established that [22], [23] the roles of B_i's are more drastic than the C_i's. On the other hand, the effects of C_i's are negligible in comparison with those of B_i's on the changes of energy consumption. Therefore, all the B_i's are logically chosen to be optimized using both the ES and GA. The B_i's are optimized subject to the following lower and upper bounds determined through the constraints:

$$\gamma = [B_1, B_2, B_3, B_4, B_5, B_6, B_7] \tag{3}$$

$$\gamma_{\min} = [68, 69, 68.5, 69, 66.5, 69.3, 69] \times 10^{-4} \tag{4}$$

$$\gamma_{\max} = [1385, 1368, 1372, 1368, 1383, 1390, 1386] \times 10^{-4} \tag{5}$$

The lower bound indicates the operational time, which we are willing to keep within t_f=8s. Note that decreasing the lower bound would yield much slower motion which is not desirable and logical, in particular for the industrial applications. The upper bound is determined based on the practical torque saturation issue such that increasing the upper bound would yield abrupt torques leading to both the motors' failures and considerably fast motion.

Therefore, the optimization problem is a constrained one, enforcing the mentioned lower and upper bounds, with the following cost function defined as the lumped amount of mechanical energy consumed in the robot:

$$\min E_{\text{tot}} = \sum_{i=1}^{7} \sum_{k=0}^{N-1} |\tau_i(k)\dot{\theta}_i(k)|\Delta t \tag{6}$$

$$\text{Subject to : The Interconnected Equations \&}$$

$$\gamma_{\min} \leq \gamma \leq \gamma_{\max}$$

We hence need to optimize seven interconnected variables using both the ES and GA. One issue to consider is the small values of the variables resulting in serious numerical errors. We fixed this problem by conditioning them using a normalization scheme as follows:

$$\gamma_n = \gamma \times 10^4 \tag{7}$$

IV. MULTIVARIABLE OPTIMIZATION USING GRADIENT-BASED EXTREMUM SEEKING

Our objective is to develop a feedback mechanism minimizing the energy consumed (E), where its nonlinear static map is known to have an extremum. We utilize the multivariable extremum seeking scheme [28]–[31], developed from Krstić and Wang efforts [2], in obtaining optimal values $B^* = [B_1^*, \cdots, B_7^*]^T$. The extremum seeking scheme estimates the gradient of cost function defined in addition to driving it to zero. The gradient is estimated using a zero-mean external periodic perturbation (or dither signal) and a series of filtering and modulation operations. The convergence of the gradient algorithm is dictated by the second derivative (Hessian) of the cost function. The minimizer is the optimal parameters B^* obtained by driving the system with a $B(l) = [B_1(l), \cdots, B_7(l)]^T$ to determine the cost value $E(l)$ and then iterating the discrete-time extremum seeking to produce the $B(l+1)$; where l denotes the l-th iteration of the algorithm [9]. Shown in Fig. 2 is a schematic of the discrete-time ES algorithm. It is worth mentioning that the measured output (Fig. 2) passing through a washout (high-pass) filter ($W(z) = \frac{z-1}{z+h}$), by having zero DC gain, expectedly helps better performance [9], [14]. Note that there is a map from the B_i's to the energy consumed (E) through Eqs. 1, 2, and 12. The extremum seeking-based optimization shown in Fig. 2 is governed by the following equations:

$$\hat{B}(l) = \frac{-\epsilon K}{z-1}[\zeta(l)] \tag{8}$$

$$\zeta(l) = M(l)\frac{z-1}{z+h}[E(l)] \tag{9}$$

$$B(l) = \hat{B}(l) + S(l) \tag{10}$$

where, $\hat{B}(l) = [\hat{B}_1(l), \cdots, \hat{B}_7(l)]^T$, ϵ is a small positive parameter, K is a positive diagonal matrix, and $h \in (0, 1)$. The $P(z)[q(l)]$ denotes the signal in the iteration domain. The perturbation signals $M(l)$ and $S(l)$ are given by

$$S(l) = \left[a_1 \cos(\omega_1 l), \cdots, a_7 \cos(\omega_7 l)\right] \tag{11}$$

$$M(l) = \left[\tfrac{2}{a_1} \cos(\omega_1 l - \phi_1), \cdots, \tfrac{2}{a_7} \cos(\omega_7 l - \phi_7)\right] \tag{12}$$

with $a_k > 0$ and the modulation frequencies are given by $\omega_k = b_k \pi$, where $|b_k| \in (0, 1)$ is a rational number and the probing frequencies are selected such that $\omega_i \neq \omega_j$ for all distinct $i, j, k \in \{1, \cdots, 7\}$. Also, phase values ϕ_k are selected such that $\mathbf{Re}\{e^{j\phi_k} W(e^{j\omega_k})\} > 0$ for all $k \in \{1, \cdots, 7\}$ [9]. Using the Taylor series expansion of the cost function around the local minimum B^* ($\nabla E(B^*) = 0$), the cost function can be written as

$$E(B) = E(B^*) + \frac{1}{2}(B - B^*)^T H (B - B^*) \tag{13}$$

where H is a positive definite Hessian matrix ($H := \frac{\partial^2 E}{\partial B^2}$). Note that cubic and higher order terms are eliminated since they are negligible for local stability analysis via averaging [14]. We then define

$$\tilde{B}(l) = \hat{B}(l) - B^* = B(l) - S(l) - B^* \tag{14}$$

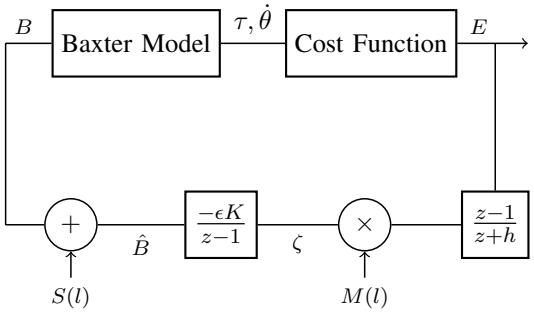

Fig. 2. Discrete-time multivariable gradient-based extremum seeking using washout filter

TABLE IV

OPTIMAL TRAJECTORIES' COEFFICIENTS

Joints's Name	Optimized B using ES	Optimized B using GA
S_0	0.0078	0.00703
S_1	0.0071	0.00700
E_0	0.1354	0.1400
E_1	0.00703	0.00700
W_0	0.01306	0.1398
W_1	0.0703	0.0650
W_2	0.1222	0.1212

Substituting Eq. 14 into Eq. 13 yields

$$E(B) = E(B^*) + \frac{1}{2}(\tilde{B} + S)^T H(\tilde{B} + S) \tag{15}$$

Eq. 8 can be rewritten as

$$\tilde{B}(l) = \frac{-\epsilon K}{z-1}[\zeta(l)] - B^* \tag{16}$$

which leads to a difference equation:

$$\begin{aligned} \tilde{B}(l+1) &= \tilde{B}(l) - \epsilon K[\zeta(l)] \\ &= \tilde{B}(l) - \epsilon K M(l) W(z)[E(l)] \end{aligned} \tag{17}$$

By substituting Eq. 15 into Eq. 17 along with using averaged system analysis, Frihauf *et al.* [9] revealed that $\tilde{B}$ locally exponentially converges to an $O(|a|)$-neighborhood of the origin through the gradient-based scheme satisfying the mentioned conditions. Therefore, $\tilde{E} = E - E^*$ locally exponentially converges to an $O(|a|^2)$-neighborhood of the origin.

V. RESULTS

We used both the analytical (ES) and numerical (GA) approaches to obtain the optimal values of B_i's shown in Figs. 3 and 4, respectively. The optimal values of B_i's are listed in Table IV indicating negligible differences between the methods. It is straightforward to observe that the optimal values of B_1, B_2, and B_4 shown in Figs. 3(a), 3(b), and 3(d), respectively, are lower than the nominal ones indicating that their corresponding links move slower than those of the nominal trajectories. This subsequently leads to a significant reduction in the energy consumed. Note that the joint S_1, as expected, takes the biggest share of energy consumption and therefore, its lower angular velocities would lead to a

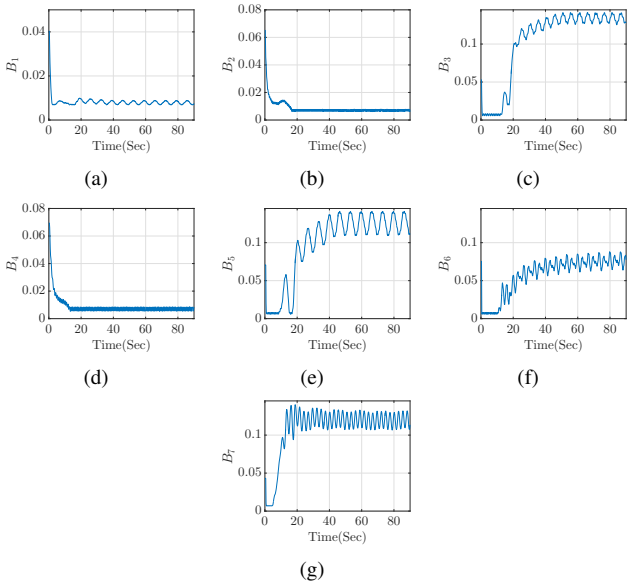

Fig. 3. The optimal values of B's using the ES

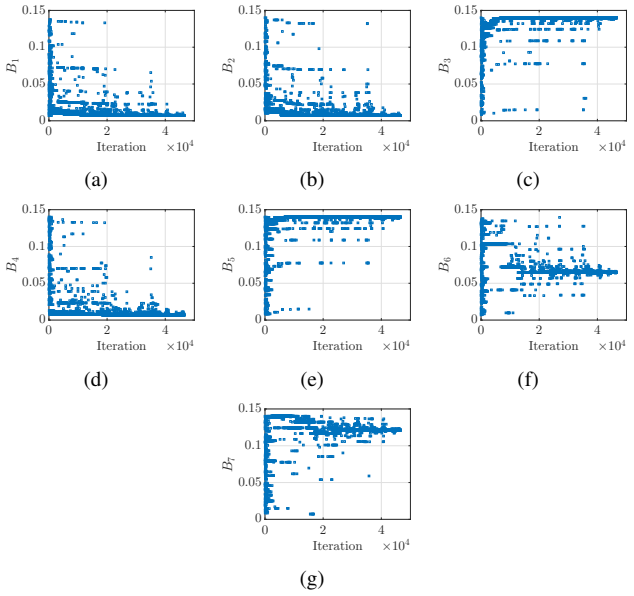

Fig. 4. The optimal values of B's using the GA

lower amount of the cost function defined. Although, the optimal values of B_3, B_5, B_6, and B_7 presented in Figs. 3(c), 3(e), 3(f), and 3(g), respectively, are higher than those of the nominal ones resulting in higher angular velocities of the optimal trajectories than the nominal ones. Shown in Figs. 5 and 6 are the energy consumptions minimized using both the ES and GA, respectively. Fig. 5(a) presents the energy optimization process versus time while the energy consumed sharply decreases to almost 37 (J) and then gradually converges to the optimal value of 36.627 (J) (at $t = 84.75$s). Shown in Fig. 5(a) reveals that the optimization of energy consumption fluctuates stochastically, as all the seven parameters (B_i's) are oscillating with seven different frequencies satisfying the mentioned conditions. Therefore, the value of optimal energy is not transparent to be compared with that of the GA one. We hence calculated its mean value

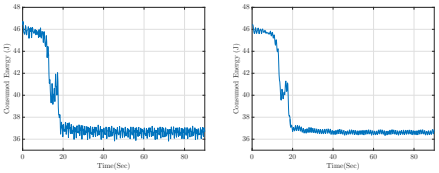

(a) (b)

Fig. 5. The (a) actual and (b) mean value of energy optimized using the ES

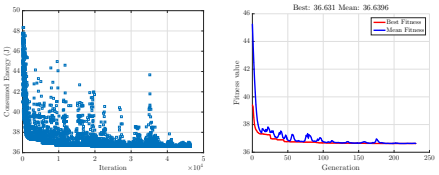

(a) (b)

Fig. 6. (a) The energy optimized using the GA and (b) the convergence history of the GA

over a running average window of one cycle of the specified fundamental low frequency (Fig. 5(b)) to obtain the amount of energy saved:

$$\Delta E_{\text{ES}} = \frac{\overbrace{E_{\text{nominal}}}^{45.34(\text{J})} - \overbrace{E_{\text{optimal}}}^{36.527(\text{J})}}{E_{\text{nominal}}} \times 100 = 19.44\% \quad (18)$$

Shown in Fig. 6(a) is the energy consumption minimized using the GA, and its best value is 36.631 (J) shown in Fig. 6(b).

$$\Delta E_{\text{GA}} = \frac{\overbrace{E_{\text{nominal}}}^{45.34(\text{J})} - \overbrace{E_{\text{optimal}}}^{36.631(\text{J})}}{E_{\text{nominal}}} \times 100 = 19.21\% \quad (19)$$

From another aspect, Fig. 6 presents considerable computational cost (iterations) of 46400 for the GA which looks logical with respect to the scale of the coupled dynamic equations resulting in a significant computational time of 2876s in comparison with 137s of the ES method. Although Figs. 5 and 6 reveal a negligible difference (less than 1%) for the energy savings of both the schemes, the ES yields the better performance. Such a superior performance of the ES can be justified as follows. The ES carries out optimization by continuously sliding on the cost function in gradient direction rather than finding optimal points discretely with a certain step size of the GA. The actual (inefficient), nominal fitted to the actual, and optimal trajectories are presented in Fig. 7 revealing the differences expected. Shown in Figs. 7(a), 7(b), and 7(d) indicate that the optimal angular velocities of joints S_0, S_1, and E_1 are lower than those of the nominal ones. The joint S_0 takes the biggest share [22], [23] among the other ones to consume the lumped amount of energy and therefore, its lower angular velocity would lead to a lower amount of the cost function defined. From another aspect, the effects of such higher values of the B_i's (i = 3, 5, 6, 7) can be visualized in Figs. 7(c), 7(e), 7(f), and 7(g), respectively. Logically, the smooth optimal trajectories shown in Figs. 7(a)-7(g), in comparison with the actual jerky ones, would expectedly demand lower driving torques to be used in the robot operation. We have also carried out experimental validation of the nonlinear analytical approach examining

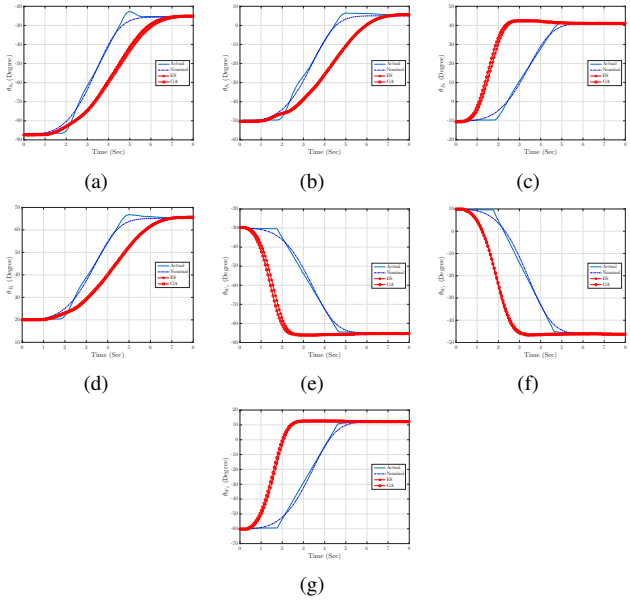

(a) (b) (c) (d) (e) (f) (g)

Fig. 7. The actual (inefficient), nominal fitted to the actual, and optimal trajectories using the ES and GA: (a) S_0; (b) S_1; (c) E_0; (d) E_1; (e) W_0; (f) W_1; (g) W_2

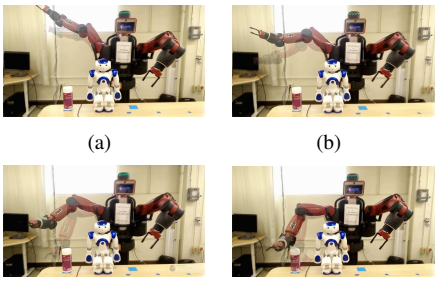

(a) (b) (c) (d)

Fig. 8. The experimental nominal and optimal trajectories using the ES in sample times of (a) t = 1s, (b) t = 3s, (c) t = 5s, and (d) t = 6s; *at t = 6s the robot's end effector through the nominal trajectory collides with another object due to the jerky motion while the optimal one avoids such a collision throughout the whole operational time*. The shadow frames present the nominal trajectory.

both the actual (inefficient) and optimal trajectories. Fig. 8 presents the experimental work, for sample operation times of 1s, 3s, 5s, and 6s, revealing smoother motions of the joints/links for the optimal path than the actual (inefficient) one. The jerky motion of the actual trajectory caused an undesirable collision between the robot's end-effector and another object at t = 6s, while the optimal one avoids such a collision throughout the whole operational time. Note that the shadow motions/frames stand for the actual (inefficient) operation. In summary, the nominal operation shown in Fig. 8 is considerably faster than the optimal one, expectedly consumes more energy, and causes the collision at t = 6s. For the optimal case, the manipulator is fast enough, moves toward the end point safely, and no jerky motion can be observed.

VI. Conclusion

Through this paper, we presented the interconnected trajectory optimization of a 7-DOF Baxter manipulator using

both the extremum seeking and heuristic based methods to avoid being trapped in several possible local minima. The coupled dynamic equations of the robot were derived utilizing the Lagrangian method and then validated through the experimental work. We then optimized the joints' trajectories to generate smooth paths to avoid being exposed to the jerky motions of the nominal ones in addition to minimizing the energy consumption. The design sensitivity analysis was then carried out to evaluate the effects of changes of the optimization variables on the cost function defined leading to select the most effective ones. Based on the sensitivity analysis, the B_i's were optimized to considerably decrease the operation's energy consumed and also to address the crucial issue of jerky motion. Finally, the optimal trajectory was experimentally implemented and compared with the actual (inefficient) one. The principal results of this research work can be summarized as follows:

- *Using the multivariable discrete-time Extremum Seeking results in a significant decrease in computational cost, an almost twenty-fold reduction relative to Genetic Algorithm.*
- A considerable amount of energy is saved (upward of 19%).
- The jerky motion and the subsequent collision between the robot's end effector and another object close to the end point are removed using the optimal trajectory, which is noted in experimental results.

REFERENCES

[1] K. B. Ariyur and M. Krstic, *Real-time optimization by extremum-seeking control*. John Wiley & Sons, 2003.

[2] M. Krstić and H.-H. Wang, "Stability of extremum seeking feedback for general nonlinear dynamic systems," *Automatica*, vol. 36, no. 4, pp. 595–601, 2000.

[3] M. Krstić, "Performance improvement and limitations in extremum seeking control," *Systems & Control Letters*, vol. 39, no. 5, pp. 313–326, 2000.

[4] H.-H. Wang, S. Yeung, and M. Krstic, "Experimental application of extremum seeking on an axial-flow compressor," *IEEE Transactions on Control Systems Technology*, vol. 8, no. 2, pp. 300–309, 2000.

[5] P. Binetti, K. B. Ariyur, M. Krstic, and F. Bernelli, "Formation flight optimization using extremum seeking feedback," *Journal of Guidance Control and Dynamics*, vol. 26, no. 1, pp. 132–142, 2003.

[6] J. Cochran, E. Kanso, S. D. Kelly, H. Xiong, and M. Krstic, "Source seeking for two nonholonomic models of fish locomotion," *IEEE Transactions on Robotics*, vol. 25, no. 5, pp. 1166–1176, 2009.

[7] J. Cochran, A. Siranosian, N. Ghods, and M. Krstic, "3-d source seeking for underactuated vehicles without position measurement," *IEEE Transactions on Robotics*, vol. 25, no. 1, pp. 117–129, 2009.

[8] A. Ghaffari, M. Krstic, and S. Seshagiri, "Power optimization and control in wind energy conversion systems using extremum seeking," *IEEE Transactions on Control Systems Technology*, vol. 22, no. 5, pp. 1684–1695, 2014.

[9] P. Frihauf, M. Krstic, and T. Başar, "Finite-horizon lq control for unknown discrete-time linear systems via extremum seeking," *European Journal of Control*, vol. 19, no. 5, pp. 399–407, 2013.

[10] C. Manzie and M. Krstic, "Extremum seeking with stochastic perturbations," *IEEE Transactions on Automatic Control*, vol. 54, no. 3, pp. 580–585, 2009.

[11] M. S. Stanković and D. M. Stipanović, "Discrete time extremum seeking by autonomous vehicles in a stochastic environment," in *Decision and Control, 2009 held jointly with the 2009 28th Chinese Control Conference. CDC/CCC 2009. Proceedings of the 48th IEEE Conference on*. IEEE, 2009, pp. 4541–4546.

[12] S.-J. Liu and M. Krstic, "Stochastic source seeking for nonholonomic unicycle," *Automatica*, vol. 46, pp. 1443–1453, 2010.

[13] S.-J. Liu and M. Krstić, "Discrete-time stochastic extremum seeking," *IFAC Proceedings Volumes*, vol. 47, no. 3, pp. 3274–3279, 2014.

[14] J.-Y. Choi, M. Krstic, K. B. Ariyur, and J. S. Lee, "Extremum seeking control for discrete-time systems," *IEEE Transactions on automatic control*, vol. 47, no. 2, pp. 318–323, 2002.

[15] M. A. Rotea, "Analysis of multivariable extremum seeking algorithms," in *American Control Conference, 2000. Proceedings of the 2000*, vol. 1, no. 6. IEEE, 2000, pp. 433–437.

[16] G. C. Walsh, "On the application of multi-parameter extremum seeking control," in *American Control Conference, 2000. Proceedings of the 2000*, vol. 1, no. 6. IEEE, 2000, pp. 411–415.

[17] K. B. Ariyur and M. Krstic, "Multivariable extremum seeking feedback: Analysis and design," in *Proc. of the Mathematical Theory of Networks and Systems*, 2002.

[18] Y. Li, M. A. Rotea, G.-C. Chiu, L. G. Mongeau, and I.-S. Paek, "Extremum seeking control of a tunable thermoacoustic cooler," *IEEE Transactions on Control Systems Technology*, vol. 13, no. 4, pp. 527–536, 2005.

[19] Y. Zhang, M. Rotea, and N. Gans, "Sensors searching for interesting things: Extremum seeking control on entropy maps," in *Decision and Control and European Control Conference (CDC-ECC), 2011 50th IEEE Conference on*. IEEE, 2011, pp. 4985–4991.

[20] Y. Zhang, J. Shen, M. Rotea, and N. Gans, "Robots looking for interesting things: Extremum seeking control on saliency maps," in *Intelligent Robots and Systems (IROS), 2011 IEEE/RSJ International Conference on*. IEEE, 2011, pp. 1180–1186.

[21] A. Ghaffari, S. Seshagiri, and M. Krstić, "Power optimization for photovoltaic micro-converters using multivariable gradient-based extremum-seeking," in *American Control Conference (ACC), 2012*. IEEE, 2012, pp. 3383–3388.

[22] M. Bagheri and P. Naseradinmousavi, "Novel analytical and experimental trajectory optimization of a 7-dof baxter robot: Global design sensitivity and step size analyses," *The International Journal of Advanced Manufacturing Technology*, vol. 93, no. 9-12, pp. 4153–4167, 2017.

[23] M. Bagheri, P. Naseradinmousavi, and R. Morsi, "Experimental and novel analytical trajectory optimization of a 7-dof baxter robot: Global design sensitivity and step size analyses," in *the ASME 2017 Dynamic Systems and Control Conference*, vol. 1, no. DSCC2017-5004, Tysons Corner, Virginia, USA, October 11-13 2017, p. V001T30A001.

[24] P. Naseradinmousavi, "A novel nonlinear modeling and dynamic analysis of solenoid actuated butterfly valves coupled in series," *ASME Journal of Dynamic Systems, Measurement, and Control*, vol. 137, no. 1, pp. 014 505–014 505–5, January 2015.

[25] P. Naseradinmousavi, D. B. Segala, and C. Nataraj, "Chaotic and hyperchaotic dynamics of smart valves system subject to a sudden contraction," *ASME. J. Comput. Nonlinear Dynam.*, vol. 11, no. 5, pp. 051 025–051 025–9, 2016.

[26] P. Naseradinmousavi, M. Bagheri, M. Krstic, and C. Nataraj, "Coupled chaotic and hyperchaotic dynamics of actuated butterfly valves operating in series," in *ASME 2016 Dynamic Systems and Control Conference*. American Society of Mechanical Engineers, 2016.

[27] P. Naseradinmousavi, M. Bagheri, and C. Nataraj, "Coupled operational optimization of smart valve system subject to different approach angles of a pipe contraction," in *ASME 2016 Dynamic Systems and Control Conference*. American Society of Mechanical Engineers, 2016.

[28] A. Ghaffari, S. Seshagiri, and M. Krstić, "Multivariable maximum power point tracking for photovoltaic micro-converters using extremum seeking," *Control Engineering Practice*, vol. 35, pp. 83–91, 2015.

[29] A. Ghaffari, M. Krstić, and S. Seshagiri, "Power optimization for photovoltaic microconverters using multivariable newton-based extremum seeking," *IEEE Transactions on Control Systems Technology*, vol. 22, no. 6, pp. 2141–2149, 2014.

[30] A. Ghaffari, M. Krstić, and D. Nešić, "Multivariable newton-based extremum seeking," *Automatica*, vol. 48, no. 8, pp. 1759–1767, 2012.

[31] K. B. Ariyur and M. Krstic, "Analysis and design of multivariable extremum seeking," in *American Control Conference, 2002. Proceedings of the 2002*, vol. 4. IEEE, 2002, pp. 2903–2908.